Radio-frequency output coupling of the Bose-Einstein condensate for atom lasers

Y. B. Band,[1] P. S. Julienne,[2] and M. Trippenbach[1]
[1]*Departments of Chemistry and Physics, Ben-Gurion University of the Negev, Beer-Sheva 84105, Israel*
[2]*Atomic Physics Division, A267 Physics, National Institute of Standards and Technology, Gaithersburg, Maryland 20899*
(Received 17 March 1998)

We develop the quantum-mechanical description of output coupling of macroscopic coherent matter waves from a Bose-Einstein condensate (BEC) via a radio-frequency field in the pulsed and cw limits for both strong and weak field coupling. The theory is converted into a Fock state description to point out the stimulated (in Bose particle) nature of the output coupling. A useful analogy with the theory of molecular photodissociation is used to explain the various regimes of output coupling BECs using radiation sources. We present specific calculations of the rates of output coupling as a function of the number of Bose atoms in the condensate and the frequency, detuning, and intensity of the radio-frequency field. [S1050-2947(99)00805-7]

PACS number(s): 03.75.Fi, 67.90.+z, 71.35.Lk

I. INTRODUCTION

Experiments have conclusively demonstrated coherence properties of Bose-Einstein condensates (BECs) [1] and the radio-frequency (rf) radiation output coupling of BECs [2]. Hence, the concept of an atom laser [3–9] based upon a BEC that is output-coupled via a rf field-stimulated process to produce macroscopic coherent matter waves has been marvelously demonstrated experimentally. In this paper we explore the nature of the output coupling for atom lasers from BECs by various types of rf radiation sources. We consider pulsed and cw atom lasers in several regimes of operation. The output coupling can be described as stimulated emission of bosonic atoms using rf radiation from a trapped spin state of the atoms in the ground state of the harmonic trap to an untrapped spin state. Our approach makes use of the strong similarity between condensate output coupling and molecular photodissociation. The condensate is analogous to a molecule which is induced to decay from a bound state into a continuum or scattering state. The analogy to photodissociation theory brings a new perspective to the different regimes of rf output coupling of BECs. Time-independent and time-dependent theories of photofragmentation have been developed in detail for many years in the chemical physics community and have full bearing on the problem of rf output coupling of BECs. Our method of description simplifies the theoretical treatment and leads to physical pictures of the dynamics based on Franck-Condon or wave-packet dynamics familiar to molecular physics. Our discussion is restricted to the case of zero temperature, where the main effect of having a condensate is to add mean-field terms to the propagation equations describing the dynamics of BEC output coupling. Generalizations to the case of finite temperature will be considered elsewhere.

The atom laser results from a transition from a trapped spin state to an untrapped one, which is no longer bound. Multicomponent (or dual) condensates have also been made [10] and studied theoretically [11–14] in which both spin components are trapped by the confining fields and therefore not outcoupled from the trap. Other recent experiments have used two-photon processes to couple different internal spin states to produce multicomponent condensates and study their relative phase [15] or time-dependent dynamics [16,17]. Optical trapping can also produce multicomponent condensates, called spinor condensates by the MIT group [18]. The molecular physics viewpoint which we develop for atom lasers can also be applied to such trapped multicomponent spin systems, and we make brief note of such possibilities.

Section II points out the analogies with molecular photoabsorption for pulsed and cw cases. Section III A reproduces the description of the impulsive limit used in Ref. [2] for the case of an intense short rf pulse, and Section III B describes how to view atom laser output coupling as a stimulated bosonic process. Section III C presents the generalized description of broadband rf output coupling which reduces in appropriate limits to the treatment in Sec. III A and to the cw treatment described in Sec. IV. Sec. V considers transitions between bound BECs. Numerical results for the weak-field narrow-band rf source case are described in Sec. VI, and a conclusion and summary are given in Sec. VII.

II. ANALOGIES WITH MOLECULAR PHOTODISSOCIATION THEORY

Let us briefly review the theory of molecular photodissociation, which involves the optical coupling of the ground electronic state of a molecule in a given vibrational-rotational state to an excited dissociative electronic state. If a broadband temporally short pulse is responsible for a molecular transition (short compared with the period of vibrational motion of the molecule), the description of the absorption process is given in terms of a time-dependent Schrödinger equation treatment of wave-packet dynamics with the transition moment operator coupling the wave-packet on the ground state to a wave-packet on the excited electronic states [19,20]. This approach is used in molecular physics to describe femtosecond chemistry experiments. Similarly, the many-body condensate at zero temperature can be viewed as a giant polyatomic molecule in a single quantum state. At the mean-field level of description of the condenstate, all the vibrational modes of the BEC (i.e., all the atomic translational degrees of freedom) are described by a single mean-field orbital, and the wave function is symmetric under interchange of the Bose particles. The vibrational fre-

quency and time scale for condensate vibration are decreased by approximately 12 orders of magnitude from the corresponding scales for ordinary molecular vibration. BEC output coupling is an rf-induced fragmentation of the condensate by a broadband temporally short rf pulse (short compared with the period of the atomic motion in the BEC trap). The time evolution is given in terms of a time-dependent wave-packet treatment with the transition moment operator coupling the wave packets for the ground and outcoupled states using a two-component time-dependent nonlinear Schrödinger equation (NLSE) [9,21]. This treatment reduces in the limit of a sufficiently intense, short rf pulse to the treatment given in [2] (see below).

In contrast to the above time-dependent picture, the usual case in molecular spectroscopy involves transitions between discrete bound states of the ground and excited manifolds induced by cw light. If a pulse is used, its duration is long compared to the time of molecular vibration. If a narrow-band, long-temporal-duration light pulse or a single-frequency cw beam is responsible for the transition, the description is best given in terms of time-independent equations for amplitudes of the vibrational states on the ground and excited electronic states that are coupled via the matter-field interaction Hamiltonian (time dependent for the case of the narrow-band pulse and time-independent for the case of the single-frequency cw source). The off-diagonal matrix elements of the Hamiltonian are those of the molecular transition dipole moment operator between the ground and excited electronic states. These molecular matrix elements, represented by $\hbar\Omega_{\rm mol}(t)$ (the Rabi frequency is not time dependent for the cw case), incorporate the effects of the transition dipole matrix element, the Franck-Condon factors between time-independent states, and the electric field strength (for an $E1$ transition) or the magnetic field strength (for an $M1$ transition). In this view, photodissociation is a weak perturbation which dissociates the molecule, on a time scale long compared with the vibrational time, with a Fermi golden rule rate which is proportional to $\Omega_{\rm mol}^2$. In the case of two optically coupled bound states, molecular Rabi oscillations occur on a time scale long compared to vibration. An analogous treatment to this molecular physics picture applies for the case of the rf outcoupling of a BEC or rf coupling of two trapped states in a BEC. The main difference is that now the dynamics is nonlinear due to the interaction of the bosons in the condensate; the nonlinear Schrödinger equation is used to determine the dynamics. Here we develop a driven equations treatment incorporating Franck-Condon factors along the lines originally drawn in molecular physics [22–26], adapted here to treat the case of rf output coupling of a BEC when the rf is applied on a time scale long compared to the vibrational period in the trap.

III. BROADBAND rf ATOM LASER

A. Intense broadband rf atom laser

The dynamics of rf coupling to a BEC was described in the limit of an intense broadband rf laser that couples different hyperfine atomic levels in Ref. [2]. The rf coupling is due to a resonant rf pulse of temporal duration $t_{\rm pulse}\ll\omega_{\rm trap}^{-1}$, where $\omega_{\rm trap}$ is the trap harmonic frequency (or suitable average frequncy for a three-dimensional anisotropic trap). A pulse with detuning Δ from rf resonance [27] couples atomic hyperfine states $|1\rangle$ and $|2\rangle$ with a coupling matrix element $\hbar\Omega/2$, where Ω is the Rabi frequency. The amplitude of these states evolves according to the Schrödinger equation:

$$i\hbar\frac{d}{dt}\begin{pmatrix}a_1\\a_2\end{pmatrix}=\hbar\begin{pmatrix}0&\Omega/2\\\Omega/2&\Delta\end{pmatrix}\begin{pmatrix}a_1\\a_2\end{pmatrix}, \tag{1}$$

State $|1\rangle$ evolves into the superposition $a_1(t)|1\rangle+a_2(t)|2\rangle$, with $a_1(t)=\cos(\Omega t/2)$ and $a_2(t)=\sin(\Omega t/2)$ for detuning $\Delta=0$. The N-particle wave function Ψ of the zero-temperature Bose condensate during and just after the rf pulse is then given by the symmetric product [2],

$$\begin{aligned}\Psi(t)&=\prod_{i=1}^{N}\phi(i,\mathbf{x},t)\\&=\sum_{N_2=0}^{N}\sqrt{\frac{N!}{(N-N_2)!(N_2)!}}a_1(t)^{N-N_2}a_2(t)^{N_2}\\&\quad\times|N-N_2,N_2\rangle,\end{aligned} \tag{2}$$

where i represents the ith particle, and the mean-field orbital ϕ is the same for all particles,

$$\phi(i,\mathbf{x},t)=\psi(\mathbf{x})[a_1(t)|1\rangle+a_2(t)|2\rangle]. \tag{3}$$

Here $\psi(\mathbf{x})$ describes the spatial shape of the initial unperturbed condensate, and the second factor describes the evolution of the internal spin states under the influence of the short, intense rf pulse. In Eq. (2), $|N-N_2,N_2\rangle$ is a state with $N_1=N-N_2$ atoms in the trapped state $|1\rangle$ and N_2 atoms in the untrapped state $|2\rangle$. For $\Delta=0$, the fraction of atoms moved out of the initial state $|1\rangle$ oscillates with the single-particle Rabi frequency Ω as $\langle N_2\rangle/N=|a_2(t)|^2=\sin^2(\Omega t/2)$, and the probability for remaining in the original ground state of the BEC is $\cos^{2N}(\Omega t/2)$. For $\Delta\neq0$, simple analytic expressions for the probabilities $|a_1(t)|^2$ and $|a_2(t)|^2$ are also well known. Experiment has shown that Eq. (2) describes the output coupling in the limit where the linewidth of the rf field, $\Delta\omega_{\rm rf}$, is large in comparison with the spacing ΔE_v between the quantized levels in the trap, $\Delta\omega_{\rm rf}\gg\Delta E_v/\hbar$ (this condition is equivalent to the statement that the rf pulse time $t_{\rm pulse}$ is short compared to the trap cycle time), and the Rabi frequency is large in comparison with the trap frequency, $\Omega\gg\omega_{\rm trap}$; thus, atoms everywhere in the trap are effectively resonant with the rf field. Equation (2) can also describe the coupling of two different bound spin states in this limit, where $|2\rangle$ is also a state trapped by the magnetic field. The physical picture behind this limit is that the fast rf pulse transforms the internal states of the atoms rapidly compared to the time scale of motion of the external center-of-mass motion of the atoms, so that no condensate motion or relaxation occurs during the pulse. Condensate relaxation occurs after the pulse is over, and the function $\psi(\mathbf{x})$ in Eq. (3) will split on a long time scale into separate pieces for each internal state 1 or 2. This is analogous to the short-pulse molecular photodissociation processes mentioned above that are used in femtosecond chemistry experiments with ordinary polyatomic molecules.

B. Stimulated bosonic processes

It should be noted that BEC output coupling is a stimulated process as far as the bosonic atoms are concerned (as is the rf transfer of population from one bound BEC state to another). It is not always evident in the one-particle picture used above where the stimulation factors occur. On the other hand, the stimulation factors are explicit in a Fock state (or number state) representation. In this section we will point out the connection between the one-particle and Fock-state viewpoints, and how the stimulation factors enter. The following analogy with the absorption of photons by atoms in an optical cavity is instructive. If the cavity modes are well established, and if optical transitions in the medium are resonant with these photons, the presence of photons populating the resonant modes stimulates the transition. For absorption or emission processes of photons of a mode populated with $n_{\rm ph}$ photons in the cavity, the probability amplitude for the process is increased by a factor of $\sqrt{n_{ph}}$ for absorption and $\sqrt{n_{\rm ph}+1}$ for emission. By analogy, for bosonic atoms initially populating a trap with all atoms in the trapped state $|1\rangle$, removing an atom from this state has an amplitude that is proportional to the square root of the number of bosons in this state. So, where is the bosonic stimulation in the atom laser theory?

Let us assume that at zero temperature the initial system is the Fock ground state for the N bosonic atoms in the rf field. Hence, initially, all atoms in the ground state occupy identical mean-field states and internal spin states $|1\rangle$. The initial state of the single BEC is given by $|N,0\rangle\Pi_{\mathbf{k}\alpha}|n_{\mathbf{k}\alpha_{\mathbf{k}}}\rangle$, where the $\mathbf{k}$ and $\alpha_{\mathbf{k}}$ are the rf photon momentum and polarization indices, and the bosonic atom Fock state $|N,0\rangle$ [see the right hand side of Eq. (2)] now takes on the meaning $|N,0\rangle = \Pi_{i=1}^{N}|1\rangle_i$. If only one field mode is present, then only one term in the product over photon field modes is nonzero. In what follows, we shall drop the photon degrees of freedom when writing matrix elements. These degrees of freedom will influence the Rabi frequency Ω; for an absorption or emission process Ω contains a factor of $\sqrt{n_{\mathbf{k}\alpha_{\mathbf{k}}}}$ or $\sqrt{n_{\mathbf{k}\alpha_{\mathbf{k}}}+1}$, respectively. In the interaction picture, after making the rotating-wave approximation, the Hamiltonian matrix elements are given by [28,29]

$$\langle N-N_2-1,N_2+1|H|N-N_2,N_2\rangle=\sqrt{(N-N_2)(N_2+1)}\hbar\Omega, \tag{4}$$

$$\langle N-N_2,N_2|H|N-N_2,N_2\rangle=N_2\hbar\Delta. \tag{5}$$

Here Δ is the rf detuning and Ω is the single-atom Rabi frequency associated with the coupling of the ground and excited atomic states by the rf field (it may or may not have Franck Condon factors depending upon the radio-frequency bandwidth; see below). The scaling of the matrix elements with the numbers of atoms in the two spin states, N_1 and N_2, follows directly from Bose-Einstein commutation relations and the properties of the condensate wave functions.

The full state of the system evolves from the initial state via the interaction with the rf pulse. The full states of the system can be represented by the $N+1$ Fock states $|N_1,N_2\rangle$ [again, the photon mode(s) are suppressed] where at any time $\langle N_1\rangle(t)+\langle N_2\rangle(t)=N$ (here the angular brackets indicate expectation value of the number operator over the state at time t). The time-dependent Schrödinger equation representing the rf coupling between the full system states can be written as a coupled set of ordinary equations for the amplitudes, $A_{N_1,N_2}(t)$. There are $N+1$ such amplitudes which can be labeled by the first number in the ket $|N_1,N_2\rangle$. These amplitudes are given (for the case of $\hbar\Delta\omega_{\rm rf}>\Delta E_v$ and $\hbar\Omega>\omega_{\rm trap}$) in the expression on the right-hand side of Eq. (2). The Schrödinger equation for the amplitudes of the Fock states labeled by α, $\{A_\alpha(t),\alpha=0,\ldots,N\}$ is given by

$$i\hbar\frac{d}{dt}A_\alpha(t)=\sum_{\beta=0}^{N}H_{\alpha,\beta}A_\beta, \tag{6}$$

where the Hamiltonian is tridiagonal, i.e., the only elements of the Hamiltonian which are nonzero are those with $\beta=\alpha\pm1$ and $\beta=\alpha$. The off-diagonal element $H_{\alpha,\beta}$ has the stimulation factor in it, i.e., $H_{\alpha,\beta}=\sqrt{\alpha\beta}\hbar\Omega/2$. For $\Delta=0$, the probability for remaining in state $|N,0\rangle$ as a function of time is $|A_{\alpha=0}(t)|^2=\cos^{2N}(\Omega t/2)$ in the limit of $\hbar\Delta\omega_{\rm rf}>\Delta E_v$ and $\hbar\Omega\gg\omega_{\rm trap}$; this probability decays from unity in time with a full width at half maximum of about N^{-1} times that of the inverse Rabi frequency. This is due to the fact that stimulation is included in the treatment, as is clearly evident from the Fock-state description. The Fock-state description is equivalent to the single-particle treatment given in Sec. III A. The description in this section is just another way of writing the equation for time evolution in a Fock basis. The Fock basis state treatment of rf coupling of different M_F states in the same F manifold, as well as the treatment of rf coupling of states in different F manifolds (either directly or via a stimulated Raman process), can be easily worked out, and will be equivalent to the treatment given above.

C. Generalized description of broadband rf atom laser

A more general description of the rf output coupling for the broadband case, $\hbar\Delta\omega_{\rm rf}>\Delta E_v$, which is valid for frequency-chirped pulses as well as constant frequency ones, whether or not the inequality $\Omega\gg\omega_{\rm trap}$ is met, is given in terms of the two-component Gross-Pitaevskii equation [9,21]:

$$\begin{aligned}i\hbar\frac{\partial}{\partial t}\psi_1(\mathbf{x},t)=&[T_{\mathbf{x}}+V_1(\mathbf{x})+U_0^{11}|\psi_1(\mathbf{x},t)|^2\\&+U_0^{12}|\psi_2(\mathbf{x},t)|^2]\psi_1(\mathbf{x},t)\\&+\frac{\hbar\Omega_0(\mathbf{x},t)}{2}\psi_2(\mathbf{x},t),\end{aligned} \tag{7}$$

$$\begin{aligned}i\hbar\frac{\partial}{\partial t}\psi_2(\mathbf{x},t)=&[T_{\mathbf{x}}+V_2(\mathbf{x})+U_0^{12}|\psi_1(\mathbf{x},t)|^2+U_0^{22}|\psi_2(\mathbf{x},t)|^2\\&+\hbar\Delta(\mathbf{x},t)]\psi_2(\mathbf{x},t)+\frac{\hbar\Omega_0(\mathbf{x},t)}{2}\psi_1(\mathbf{x},t).\end{aligned} \tag{8}$$

Here $T_{\mathbf{x}}$ is the kinetic energy operator and $U_0^{ij}=(4\pi\hbar^2/m)NA_0^{ij}$ are the atom-atom interaction strengths, proportional to the s-wave scattering lengths A_0^{11}, A_0^{22}, and A_0^{12} for collisions of atomic states $1+1$, $2+2$, and $1+2$,

respectively, and Ω_0 denotes the Rabi frequency coupling atomic states 1 and 2. We assume that the scattering lengths are real, that is, inelastic collisional processes do not contribute any loss processes. For generality, we have allowed for the possibility that the Rabi frequency and the detuning can be time and space dependent in Eqs. (7) and (8). In what follows, we shall not make use of this full generality, i.e., for simplicity we take these quantities to be independent of space while the rf pulse is on.

In the limit that the rf pulse time $t_{\rm pulse}$ is short compared to the trap cycle time and the Rabi frequency Ω_0 is large, this treatment yields the same oscillatory behavior as the dynamics described above in Sec. III A. In this limit, the solution to the two-component Gross-Pitaevskii equation can be taken as $\psi_1(\mathbf{x},t)=a_1(t)\psi(\mathbf{x})$, $\psi_2(\mathbf{x},t)=a_2(t)\psi(\mathbf{x})$ with $\psi(\mathbf{x})$ being the initial BEC solution to the Gross-Pitaevskii equation at $t=0$. Substituting these forms for $\psi_j(\mathbf{x},t)$ into Eqs. (7) and (8) and taking the inner product with $\psi(\mathbf{x})$ yields a set of coupled equations for $a_1(t)$ and $a_2(t)$ which, as we now demonstrate, is equivalent to Eq. (1). We first introduce phase factors in the definition of $a_j(t)$ by taking $a_j(t)=b_j(t)\exp(-i\int^t dt'\,\phi_j(t'))$, where $\phi_j(t)$ will be defined shortly. Furthermore, we introduce time-dependent coefficients $U^j(t)=\Sigma_{k=1}^2 U_0^{j,k}|a_k(t)|^2$. We now define the time-dependent phases $\phi_j(t)$ as the following expectation values:

$$\phi_j(t)=\frac{1}{\hbar}\int d^3x\,\psi^*(\mathbf{x})[T_{\mathbf{x}}+V_j(\mathbf{x})+U^j(t)|\psi(\mathbf{x})|^2]\psi(\mathbf{x}). \tag{9}$$

Substituting the forms for $\psi_j(\mathbf{x},t)$ and using the assumption that $\int_0^t dt'[\phi_1(t')-\phi_2(t')]$ can be neglected on the time scale $t\ll t_{\rm pulse}$, we obtain the set of coupled equations, for $b_j(t)$,

$$i\hbar\frac{d}{dt}\begin{pmatrix}b_1\\ b_2\end{pmatrix}=\hbar\begin{pmatrix}0 & \Omega_0/2\\ \Omega_0/2 & \Delta\end{pmatrix}\begin{pmatrix}b_1\\ b_2\end{pmatrix}. \tag{10}$$

Equation (10) gives the same probabilities as Eq. (1).

IV. NARROW-BAND rf ATOM LASER

For $\hbar\Delta\omega_{\rm rf}<\Delta E_v$, only one (or a small number) of the vibrational states in the trap can be excited. The theoretical treatment is best composed in a time-independent formulation similar to the treatment used in molecular spectroscopy with narrowband laser sources [23], or the treatment of predissociation of a molecular level into a dissociative continuum state [22]. In this regime, a steady-state (cw) atom laser can be created, if the rate of loss of population of the BEC via output coupling is compensated for by pumping (cooling) atoms into the BEC. Provided the output coupling rate $W_{\rm oc}$ is small, namely, $W_{\rm oc}\ll\omega_{\rm trap}$, the following perturbation theory expression for the rate of output coupling is valid:

$$W_{\rm oc}=\frac{2\pi}{\hbar}|T|^2, \tag{11}$$

where $T=(\hbar\Omega_0/2)\langle E|v_g\rangle$. The radio-frequency is sufficiently low that the plane-wave factor(s) of $\exp(i\mathbf{k}_{\rm rf}\cdot\mathbf{r}_i)$ originating from the electromagnetic field operator do not have to be included in the matrix element [28]. The Franck-Condon amplitude $\langle E|v_g\rangle$ appearing in the transition matrix T is a free-bound overlap integral of the continuum output coupled state and the ground-state BEC wave function. [A similar bound-bound overlap integral will be defined in Eq. (28) below for the case of coupling of two different bound spin states.]

Equation (11) can be derived by considering the time-independent nonlinear Schrödinger equation derived from Eqs. (7) and (8):

$$[T_{\mathbf{x}}+V_1(\mathbf{x})-\mu+U_0^{11}|\psi_1|^2+U_0^{12}|\psi_2|^2]\psi_1(\mathbf{x})+(\hbar\Omega_0/2)\psi_2(\mathbf{x})=0, \tag{12}$$

$$[T_{\mathbf{x}}+V_2(\mathbf{x})+U_0^{12}|\psi_1|^2+U_0^{22}|\psi_2|^2+\hbar\Delta-\mu]\psi_2(\mathbf{x})+(\hbar\Omega_0/2)\psi_1(\mathbf{x})=0, \tag{13}$$

where μ is the chemical potential of the BEC. Using the assumption of weak coupling, where the amplitude of the outcoupled wave ψ_2 remains small compared to the amplitude of the trapped state ψ_1, Eqs. (12) and (13) can be treated by perturbation theory as follows. Set $U_0^{22}|\psi_2|^2=0$ on the left hand side of Eq. (13) to obtain

$$[T_{\mathbf{x}}+V_2(\mathbf{x})+U_0^{12}|\psi_1|^2+\hbar\Delta-\mu]\psi_2(\mathbf{x})+(\hbar\Omega_0/2)\psi_1(\mathbf{x})=0, \tag{14}$$

and let ψ_1 in this resulting equation satisfy the *undriven* equation obtained by setting $\Omega_0=0$ and $U_0^{12}|\psi_2|^2=0$ in Eq. (12). The driven equation (14) for ψ_2 can be written as an integral equation in terms of the Green's function for the excited state. That is, the driven Schrödinger equation (14) can be solved to obtain ψ_2, by converting it to an integral equation, and the asymptotic form of ψ_2 is proportional to the transition matrix. This is demonstrated in the next two subsections for the 1D and spherically symmetric cases, respectively.

A. Narrow-band 1D model

For the 1D case, Eq. (14) yields the integral equation

$$\psi_2(x)=\int_{-\infty}^{+\infty}dx'\,G(\mu-\hbar\Delta;x,x')\hbar\Omega_0/2\psi_1(x'), \tag{15}$$

where the Green's function $G(\mu-\hbar\Delta;x,x')$ is given by

$$G(\mu-\hbar\Delta;x,x')=(\mu-\hbar\Delta-H)^{-1}=h^+(x_<)W(h^-,h^+)^{-1}h^+(x_>), \tag{16}$$

and $x_<=\min(x,x')$ and $x_>=\max(x,x')$. The asymptotic form of the Green's function is such that $\psi_2(x)\to Th^+(x)$ for large positive x with $h^+(x)$ having only right-outgoing contributions for large positive x, and incoming and outgoing contributions for large negative x. The transition amplitude is given by [24–26]

$$T=\frac{\hbar\Omega_0/2}{W(h^-,h^+)}\int_{-\infty}^{+\infty}dx'\,h^-(x')\psi_1(x'), \tag{17}$$

and the Wronskian is $W(h^-,h^+)=2ik=2i\sqrt{2m(\mu-\hbar\Delta)/\hbar}$. The wave function $h^-(x)$ satisfies the equation

$$\left(\frac{-\hbar^2}{2m}\frac{d^2}{dx^2}+V_2(x)+U_0^{12}|\psi_1|^2+\hbar\Delta-\mu\right)h^-(x)=0, \tag{18}$$

and has only outgoing waves to the left (large negative x). The integral in Eq. (17) can be approximated for positive scattering length cases with large numbers of bosons by taking the Thomas-Fermi approximation for ψ_1, obtained by neglecting the kinetic energy in the time-independent nonlinear Schrödinger equation for ψ_1 [30]:

$$\psi_1(x)=\sqrt{\frac{\mu-V_1(x)}{U_0^{11}}} \tag{19}$$

for values of x, where $\mu-V_1(x)>0$ is positive and $\psi_1(x)=0$ otherwise. For values of x for which the square root expression for ψ_1 is positive, Eq. (18) can be approximated by

$$\left(\frac{-\hbar^2}{2m}\frac{d^2}{dx^2}+V_2(x)-\frac{U_0^{12}}{U_0^{11}}V_1(x)+\frac{U_0^{12}}{U_0^{11}}\mu+\hbar\Delta\right)h^-(x)=0. \tag{20}$$

The integral can be calculated numerically by quadrature or an invariant imbedding method can be used to calculate the transition amplitude [25].

B. Narrow-band spherically symmetric model

For the spherically symmetric case, the asymptotic form of $\psi_2(\mathbf{x})$ is $Th^+(\mathbf{x})$, where T is the transition amplitude and $h^+(\mathbf{x})$ contains only an outgoing wave contribution asymptotically [25,26]. More specifically, the angular part of the final driven wave function $\psi_2(\mathbf{x})$ is isotropic, and the radial part, $\chi_2(r)$, satisfies the equation

$$\chi_2(r)=\hbar\Omega_0/2\int_0^\infty dr' G(\mu-\hbar\Delta;r,r')\chi_1(r'), \tag{21}$$

where $\chi_1(r)=\sqrt{4\pi}r\psi_1(r)$ and $\chi_2(r)=\sqrt{4\pi}r\psi_2(r)$. The Green's function $G(\mu-\hbar\Delta;r,r')$ is given by

$$\begin{aligned}G(\mu-\hbar\Delta;r,r')&=(\mu-\hbar\Delta-H)^{-1}\\&=s(r_<)W(s,h^+)^{-1}h^+(r_>),\end{aligned} \tag{22}$$

where $r_<=\min(r,r')$ and $r_>=\max(r,r')$. The asymptotic form of $\psi_2(r)$ is $Th^+(r)$ with the transition amplitude given by [25]

$$T=\frac{\hbar\Omega_0/2}{W(s,h^+)}\int_0^{+\infty}dr' s(r')\chi_1(r'), \tag{23}$$

where $W(s,h^+)=-1$, and the regular radial wave function $s(r)$ satisfies the equation

$$\left(\frac{-\hbar^2}{2m}\frac{d^2}{dr^2}+V_2(r)+U_0^{12}|\psi_1|^2+\hbar\Delta-\mu\right)s(r)=0. \tag{24}$$

Equation (23) can be approximated by making the Thomas-Fermi approximation for $\chi_1(r)$. Here, too, the integral in Eq. (23) can be calculated numerically by quadrature or an invariant imbedding method can be used to calculate the transition amplitude [25].

In setting up the spherically symmetric problem, it should be remembered that the wave function ψ_1 is written as $\psi_1=[\chi_1(r)/r](1/\sqrt{4\pi})$. Hence the equation for the uncoupled bound-state radial wave function is given by

$$\left[\frac{-\hbar^2}{2m}\frac{d^2}{dr^2}+V_1(r)+\left(\frac{U_0^{11}}{4\pi}\right)\left|\frac{\chi_1(r)}{r}\right|^2+\hbar\Delta-\mu\right]\chi_1(r)=0. \tag{25}$$

The coefficient of the nonlinear term in the radial equation is divided by 4π, and the nonlinear term contains a factor of r^{-2}. Note that $\chi_1(r)/r$ is finite at the origin and $\chi_1(r)$ vanishes at the origin, similarly for the coupled radial equations.

V. rf TRANSITIONS BETWEEN BOUND BECs

The treatment for bound-bound transitions (two bound condensates of different atomic spin states that are *both* bound) can also be considered in the narrow-band and broad-band rf transition limits. In the regime where $\hbar\Delta\omega_{\rm rf}<\Delta E_v$ and the Rabi frequency Ω_0 is small, the transition rates can be well approximated by a perturbation theory treatment which results in an equation similar to Eq. (23), except that the generalized Rabi frequency appearing in the new equation is given by

$$\Omega=\Omega_0\langle v_e|v_g\rangle. \tag{26}$$

Ω contains a bound-bound overlap integral rather than the free-bound overlap integral appearing in Eq. (23). The bound-bound overlap integral for the mean-field motion of the atoms corresponds to what is known as the bound-bound Franck-Condon factor in the case of molecular transitions induced by cw light fields. Here the transition is between well defined quantum states of internal (spin) and external (coordinate) degrees of freedom. Hence, for cw rf sources coupling bound spin states, the actual frequency in the dynamics, Ω, can be much smaller than Ω_0.

The regime of $\hbar\Delta\omega_{\rm rf}\gg\Delta E_v$ and $\Omega_0\gg\omega_{\rm trap}$ results in an equation identical to Eq. (1) for the time dynamics is given by

$$i\hbar\frac{d}{dt}a_1(t)=(\hbar\Omega_0/2)a_2(t), \tag{27}$$

$$i\hbar\frac{d}{dt}a_1(t)=\hbar\Delta a_2(t)+(\hbar\Omega_0/2)a_1(t). \tag{28}$$

In this impulsive limit where the time evolution occurs in a time short compared to $\omega_{\rm trap}^{-1}$, the subsequent relaxation of

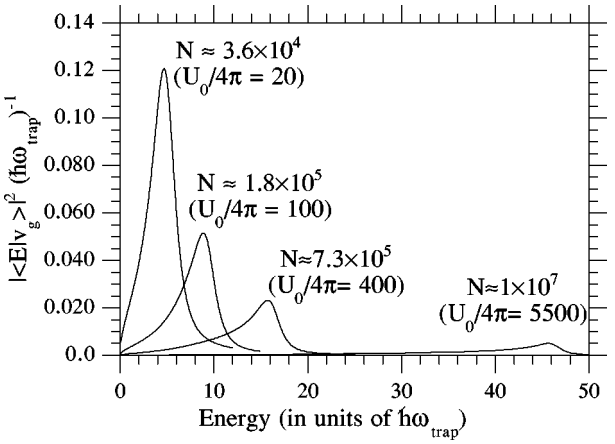

FIG. 1. Bound-free Franck-Condon factor, $|\langle E|v_g\rangle|^2 = |T|^2/(\hbar\Omega_0/2)^2$ versus the asymptotic kinetic energy of the BE particles E $(=\mu-\hbar\Delta$, where Δ is the detuning of the rf from producing output particles at kinetic energy $\mu)$ for the four values of $N\approx 3.6\times 10^4$, 1.8×10^5, 7.3×10^5, and 1.0×10^7.

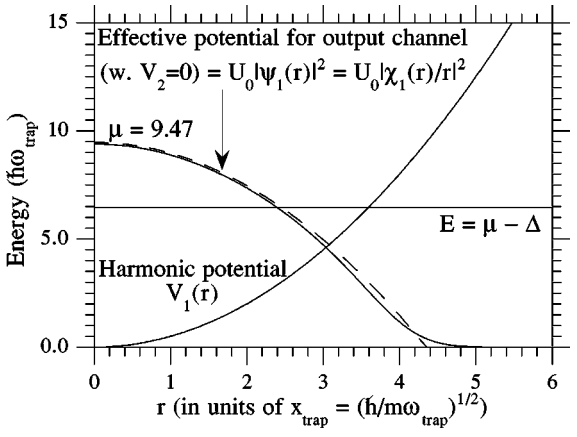

FIG. 2. Effective repulsive potential, $V_2(r)+U_0|\psi_1|^2$ for $\mu = 9.47\hbar\omega_{\rm trap}$ and harmonic potential $V_1(r)$ versus radial distance r.

the spatial part of the condensate wave function can be calculated from Eqs. (7) and (8), where $\Omega_0=0$ and the initial conditions for the two components are $\psi_1(\mathbf{x},t=t_{\rm pulse}) = a_1(t_{\rm pulse})\psi_1(\mathbf{x},t=0)$ and $\psi_2(\mathbf{x},t=t_{\rm pulse})=a_2(t_{\rm pulse})\psi_1(\mathbf{x},t=0)$, where $\psi_1(\mathbf{x},t=0)$ is the ground-state solution to the time-independent Gross-Pitaevskii equation for the single-component trap.

A more general description of the rf transitions between bound BECs for the case of $\hbar\Delta\omega_{\rm rf}>\Delta E_v$, which is valid whether or not the inequality $\Omega_0\gg\omega_{\rm trap}$ is true, is given by a treatment identical to that in Sec. III C.

VI. NUMERICAL RESULTS FOR WEAK-FIELD NARROWBAND OUTPUT COUPLING

We present results of calculations for the rate of output coupling using the narrow-band spherically symmetric model for a ^{23}Na BEC, with $A_0=52a_0$ [31] ($a_0=0.0529$ nm) and $x_r=\sqrt{\hbar/m\omega_{\rm trap}}=5$ μm. The escaping particles are taken to have $m_F=0$, so the repulsive potential $V_2(r)=0$. We shall assume $A_0^{11}=A_0^{22}=A_0^{12}$, so only one atom-atom interaction strength, U_0, occurs in our calculation. We consider $U_0/(4\pi)=20$, 100, 400, and 5500 for which $N\approx 3.6\times 10^4$, 1.8×10^5, 7.3×10^5, and 1.0×10^7 atoms, respectively. The calculated chemical potentials for these numbers of atoms are approximately $\mu=5.15$, 9.47, 16.4, and $46.3\hbar\omega_{\rm trap}$, respectively. The transition amplitude is computed using Eq. (23) and the rate for output coupling is determined using Eq. (11). Our calculations were carried out using the numerically computed BEC ground state computed via a fast Fourier transform split operator method similar to the one used in Refs. [32–35], and the nonlinear eigenvalue and eigenfunction of the time-independent NLSE are obtained by turning time into imaginary time in the time-dependent NLSE and letting the solution relax to the ground state.

Figure 1 shows the free-bound Franck-Condon factor, $|\langle E|v_g\rangle|^2=|T|^2/(\hbar\Omega_0/2)^2$, versus asymptotic kinetic energy E of the bosons $(E=\mu-\hbar\Delta)$ for the four values of N used $[\langle E|v_g\rangle\equiv\int_0^{+\infty}dr' s_E(r')\chi_1(r')]$. Note that as the frequency $\omega_{\rm rf}$ changes (i.e., as the detuning Δ changes), the asymptotic kinetic energy E of the ouput coupled particles changes. E is fully determined in terms of $\omega_{\rm rf}$, hence the distribution of energy E would be a δ function with $E=\mu-\Delta$ were it not for the finite output coupling rate (which determines the linewidth). Our calculated results are valid provided $W_{\rm oc}\ll 1$.

The maximum of the Franck-Condon factor (i.e., the maximum of $W_{\rm oc}$) occurs for values of $E\approx\mu$ and just slightly less than μ. The falling off of the Franck-Condon factor for E away from μ is clearly illustrated in Fig. 1. This dependence on E can be understood as follows. Figure 2 shows a number of potentials; the effective attractive ground-state potential is given by $V_1(r)+U_0|\psi_1|^2$ and the effective repulsive potential for the final state is given by the sum $V_2(r)+U_0|\psi_1|^2$ which equals $U_0|\psi_1|^2$ since $V_2(r)=0$. In the Thomas-Fermi (TF) approximation the effective attractive ground-state potential is μ for $0\leqslant r\leqslant x_{\rm TF}$ and is harmonic for $r>x_{\rm TF}$, where $x_{\rm TF}=\sqrt{2\mu/m\omega_{\rm trap}^2}$ is the TF radius. The integrand for the overlap integral which defines the free-bound Franck-Condon factor is the product $s_E(r)\chi_1(r)$, where the free wave function $s_E(r)$ for $E=\mu-\Delta$ is determined from the repulsive potential and the bound wave function $\chi_1(r)$ is determined from the attractive potential. The effective repulsive potential in Fig. 2 is shown using both the TF approximation and the exact (numerically computed) BEC ground state. The line at $E=\mu-\Delta$ in the figure crosses this repulsive potential at the classical turning point for motion on this potential. If $E\approx\mu$, this classical turning point, or Condon point, is near $r=0$. The Condon point varies from large r to $r=0$ as E varies from 0 to μ, and a real Condon point no longer exists for $E>\mu$. The latter case defines a classically forbidden Franck-Condon factor, which drops off exponentially with increasing E, like an antistatic wing of a pressure broadened transition. When the rf is tuned so that the final-state energy E is in the range $0<E<\mu$, there is a real Condon crossing point for the effective repulsive potential. When the rf is tuned so that the final-state energy $E>\mu$, there is no longer a real crossing point, and the integral decays exponentially with increasing E.

The output coupling rate per particle is given by Eq. (11) as

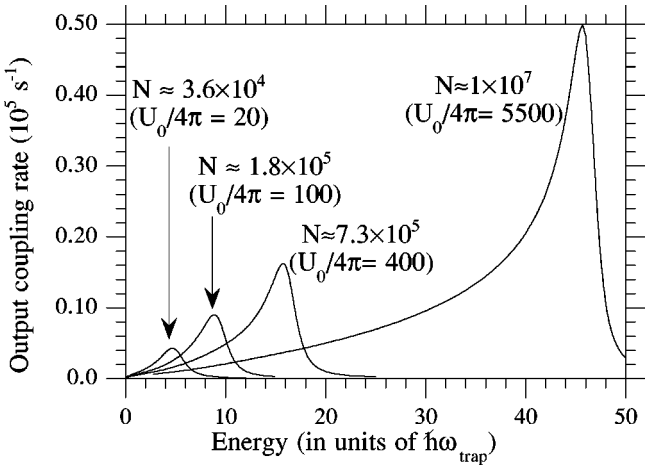

FIG. 3. Total BEC output coupling rate versus asymptotic kinetic energy of the bosons for the four values of $N \approx 3.6 \times 10^4$, 1.8×10^5, 7.3×10^5, and 1.0×10^7. We have arbitrarily taken the coupling strength such that $\hbar\Omega_0^2/4 = 1$ in Eq. (29).

$$W_{\mathrm{oc}} = \frac{2\pi}{\hbar}\left|\frac{\hbar\Omega_0}{2}\langle E|v_g\rangle\right|^2 = \frac{\hbar\Omega_0^2}{4}|\langle E|v_g\rangle|^2. \tag{29}$$

The total BEC output coupling rate is given by

$$W_{\mathrm{BEC,out}} = NW_{\mathrm{oc}} \tag{30}$$

and is plotted in Fig. 3 versus asymptotic kinetic energy E for the four values of N that we have taken. Clearly the output coupling rate $W_{\mathrm{BEC,out}}$ for each value of N peaks at the same value of energy as W_{oc}; the energy of the peak as well as the peak output coupling rate increase with increasing N. Moreover, the width of the energy distribution becomes narrower with increasing N.

The interpretation of Fig. 3 is as follows. As the rf frequency changes, the output coupling rate changes. The energy distribution of the output coupled particles would be a δ function at the kinetic energy determined by the rf frequency ω_{rf}, i.e., the energy of the output particles would be completely determined for a given rf frequency, were it not for the fact that the output coupling rate is finite. The width of the kinetic energy distribution at a given kinetic energy E ($E = \mu - \Delta$) is related (but not equal) to the inverse of the calculated output coupling rate at this energy. The width will change with time [36], because the nature of the BEC changes with time (if it is not replenished by continued evaporative cooling), much like the width of the fluorescence spectrum of a large molecule changes with time because of the relaxation of the molecule over times short compared with the decay time.

In order to check the validity of using the TF approximation in the calculation of the free-bound overlap integral, we compare in Fig. 4 the results of computing the integral using TF and the numerically computed BEC ground-state wave function. At high energies the results using TF are very accurate. At very low energies, the TF results in somewhat smaller values of the integral. This occurs because the exact continuum wave function is larger around the true turning point than the TF, and the bound-state wave function is larger at this turning point than the turning point for the TF

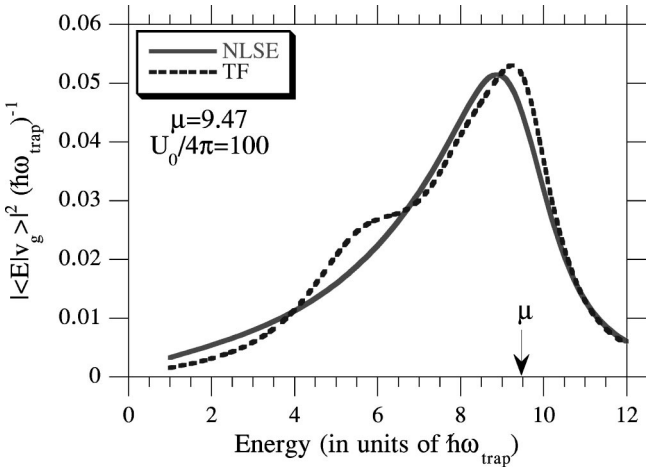

FIG. 4. Bound-free Franck-Condon factor versus energy computed using the Thomas-Fermi approximation and the numerically computed BEC ground-state wave function.

(see Fig. 5). In the intermediate energy regime, from about 4 to 6 $\hbar\omega_{\mathrm{trap}}$, the integral calculated using TF is somewhat larger than the results using the exact wave function because the TF wave function is larger at the classical turning point on the effective repulsive potential.

The criterion for a cw atom laser is that the time for the atoms to leak out into the output coupled state must be long compared to the oscillation period in the trap, that is,

$$W_{\mathrm{oc}} \ll \omega_{\mathrm{trap}}. \tag{31}$$

VII. SUMMARY AND CONCLUSIONS

The theory of atom laser output coupling for cw or weak narrow-band rf fields and pulsed broadband rf fields is best developed using time-independent and time-dependent treatments, respectively (in analogy with the theory of photodissociation of molecules discussed in Sec. II). We developed a general framework in which to describe atom laser output coupling of BECs, and showed how this theory reduced in the limit of cw rf fields and the limit of intense broadband

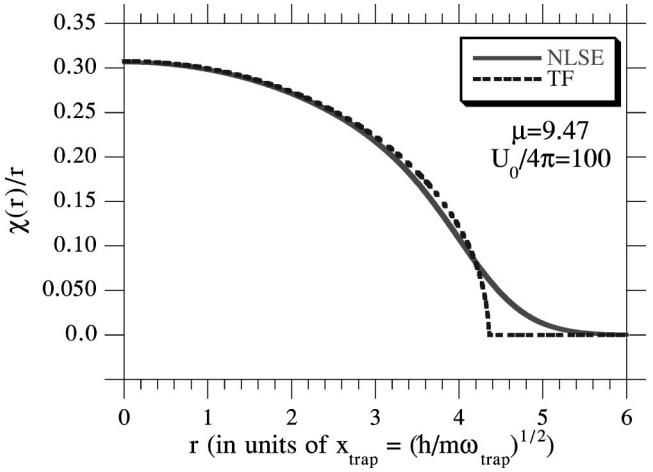

FIG. 5. Ground-state wave function versus r computed using the Thomas-Fermi approximation and the numerically computed BEC ground-state wave function.

fields to much simpler formulations. We presented numerical results for the output coupling rate versus rf detuning and number of atoms in the BEC for narrow-band weak rf fields. We find that (a) the rate is largest for $E \approx \mu$ (i.e., largest for zero detuning and decreases for both positive and negative detuning), (b) the rate increases at a rate less than linear with the number of particles, (c) the width of the energy distribution becomes narrower with increasing N. The reasons for these trends are that (i) for an energy $E \approx \mu$, the classical turning point is near $r=0$, so one expects good overlap of the continuum wave function with the ground-state BEC wave function, and for energies lower or higher than $E \approx \mu$ the overlap integral decreases, and (ii) the maximum of the free-bound overlap integral (supremum over energy) decreases with N and the width of the distribution of energies as determined by $W_{\rm oc}$ becomes narrower. In the limit of $\hbar\Delta\omega_{\rm rf} > \Delta E_v$ and $\hbar\Omega \gg \omega_{\rm trap}$, and for $\Delta=0$, the probability of finding output coupled particles as a function of time is given by $1-P_{N,0}(t)=1-\cos^{2N}(\Omega t/2)$, where t is the time duration for which the rf field is on. An analytic expression for the probability can also be easily worked out in this limit for $\Delta \neq 0$ in terms of the generalized Rabi frequency $\Omega' = \sqrt{\Delta^2+\Omega^2}$. For weaker Rabi frequencies, the temporal behavior is more complicated and must be calculated using the two-component Gross-Pitaevskii equation [9,21]. Stimulation due to the population of states by the bosonic atoms is explicitly included in the treatment, as is clearly evident from the Fock-state description presented in Sec. III B.

For rf-induced transitions between bound levels of different hyperfine structure states, the nature of the formulation again depends on the linewidth of the rf field as compared with the spacing between the mean-field bound-state levels. If the bandwidth is small compared with the spacing between levels, the time dependence of the amplitude of individual mean-field eigenstates due to the presence of the rf field is determined, whereas if the bandwidth is large compared with the spacing between levels, one calculates the amplitudes of the hyperfine levels without explicitly determining the population of the mean-field bound-state eigenstates.

The treatment here has been developed for zero-temperature BECs at the level of a Hartree mean-field approximation. This treatment can be generalized to finite temperatures where it is essential to include the above mean-field contribution to BEC (even at zero temperatures there will be a very small contribution from the above mean-field contribution in a more complete theory). For the finite-temperature case, a density-matrix generalization (including the above mean-field contribution) of the theory presented here can be readily developed.

Our treatment can also be easily generalized to Raman output coupling schemes to couple states that differ by two or zero units of azimuthal quantum number and angular momentum quantum number, wherein pump and Stokes rf fields induce Raman hyperfine transitions (the intermediate state of the Raman process can be off-resonant).

ACKNOWLEDGMENTS

This work was supported in part by grants from the U.S.-Israel Binational Science Foundation, the James Franck Binational German-Israel Program in Laser-Matter Interaction (Y.B.B.), and the U.S. Office of Naval Research (P.S.J.). We thank Mark Edwards, Bill Phillips, Yonathan Japha, and Kalle-Antti Suominen for valuable discussions.

[1] M. O. Mewes *et al.*, Phys. Rev. Lett. **77**, 988 (1996).
[2] M. O. Mewes *et al.*, Phys. Rev. Lett. **78**, 582 (1997).
[3] M. J. Holland *et al.*, Phys. Rev. A **54**, R1757 (1996).
[4] G. M. Moy and C. M. Savage, Phys. Rev. A **56**, R1087 (1997).
[5] H. Wiseman, A. Martins, and D. Walls, Quantum Semiclassic. Opt. **8**, 737 (1996).
[6] J. J. Hope, Phys. Rev. A **55**, R2531 (1997).
[7] A. M. Guzman *et al.*, Phys. Rev. A **53**, 977 (1996).
[8] R. J. C. Spreeuw *et al.*, Europhys. Lett. **32**, 469 (1995).
[9] R. J. Ballagh, K. Burnett, and T. F. Scott, Phys. Rev. Lett. **78**, 3276 (1997).
[10] C. J. Myatt, E. A. Burt, R. W. Ghrist, E. A. Cornell, and C. E. Wieman, Phys. Rev. Lett. **78**, 586 (1997).
[11] T.-L. Ho and V. B. Shenoy, Phys. Rev. Lett. **77**, 3276 (1996).
[12] B. D. Esry, C. H. Greene, J. P. Burke, and J. L. Bohn, Phys. Rev. Lett. **78**, 3594 (1997).
[13] P. Öhberg and S. Stenholm, Phys. Rev. Lett. **57**, 1272 (1998).
[14] H. Pu and N. P. Bigelow, Phys. Rev. Lett. **80**, 1130 (1998).
[15] D. S. Hall, M. R. Matthews, C. E. Wieman, and E. A. Cornell, Phys. Rev. Lett. **81**, 1543 (1998).
[16] M. R. Matthews, D. S. Hall, D. S. Jin, J. R. Ensher, C. Wieman, E. A. Cornell, F. Dalfovo, C. Minniti, and S. Stringari, Phys. Rev. Lett. **81**, 243 (1998).
[17] D. S. Hall, M. R. Matthews, J. R. Ensher, C. E. Wieman, and E. A. Cornell, Phys. Rev. Lett. **81**, 1539 (1998).
[18] J. Stenger, S. Inouye, D. M. Stamper-Kurn, H.-J. Miesner, A. P. Chikkatur, and W. Ketterle, Nature (London) **396**, 345 (1998).
[19] E. J. Heller, J. Chem. Phys. **62**, 1544 (1975); **68**, 3891 (1978); K. C. Kulander and E. J. Heller, *ibid.* **69**, 2439 (1978); K. C. Kulander, Comput. Phys. Commun. **63**, 1 (1991).
[20] E. Geva and R. Kosloff, J. Chem. Phys. **102**, 8541 (1995); R. Kosloff, *ibid.* **92**, 2087 (1988).
[21] H. Wallis, A. Rohrl, M. Naraschewski, and A. Schenzle, Phys. Rev. A **55**, 2109 (1997).
[22] P. S. Julienne and M. Krauss, J. Mol. Spectrosc. **56**, 270 (1975).
[23] S. J. Singer, K. F. Freed, and Y. B. Band, J. Chem. Phys. **77**, 1942 (1982); S. J. Singer, K. F. Freed, and Y. B. Band, *Advances In Chemical Physics, Vol. LXI* (John Wiley, New York, 1985), pp. 1–114, and references therein.
[24] Y. B. Band and I. Tuvi, J. Chem. Phys. **100**, 8869 (1994); I. Tuvi, Y. Avishai, and Y.B. Band, J. Phys.: Condens. Matter **7**, 604 (1995).
[25] S. J. Singer, K. F. Freed, and Y. B. Band, J. Chem. Phys. **77**, 1942 (1982).
[26] I. Tuvi and Y. B. Band, J. Chem. Phys. **99**, 9697 (1993); Y. B. Band and I. Tuvi, *ibid.* **99**, 9704 (1993).

[27] Δ is the detuning of the central radio-frequency from producing output particles at kinetic energy μ. The resonance condition is satisfied at all points in the condensate for the case in Ref. [2] where the frequency width of the rf pulse is very broad and one can take $\Delta = 0$.
[28] Y. B. Band, Phys. Rev. A **54**, 1500 (1996).
[29] P. Bouyer and M. A. Kasevich, Phys. Rev. A **56**, R1083 (1997).
[30] M. Edwards and K. Burnett, Phys. Rev. A **51**, 1382 (1995); G. Baym and C. Pethick, Phys. Rev. Lett. **76**, 6 (1996).
[31] E. Tiesinga, C. J. Williams, P. S. Julienne, K. M. Jones, P. D. Lett, and W. D. Phillips, J. Res. Natl. Inst. Stand. Technol. **101**, 505 (1996).
[32] M. Trippenbach and Y. B. Band, Phys. Rev. A **56**, 4242 (1997).
[33] M. Trippenbach and Y. B. Band, Phys. Rev. A **57**, 4791 (1998).
[34] Y. B. Band and M. Trippenbach, Phys. Rev. Lett. **76**, 1457 (1996); M. Trippenbach and Y. B. Band, J. Opt. Soc. Am. B **13**, 1403 (1996); C. Radzewicz, J. S. Krasinski, M. J. la Grone, M. Trippenbach, and Y. B. Band, *ibid.* **14**, 420 (1997).
[35] M. Trippenbach, T. C. Scott, and Y. B. Band, Opt. Lett. **22**, 579 (1997).
[36] Y. Japha, S. Choi, K. Burnett, and Y. B. Band, Phys. Rev. Lett. **82**, 1079 (1999).